Research Article

Mahesh Attimarad*, Katharigatta Narayanaswamy Venugopala, Anroop B. Nair, Bandar Aldhubiab, and Sreeharsha Nagaraja

In silico modified UV spectrophotometric approaches to resolve overlapped spectra for quality control of rosuvastatin and teneligliptin formulation

https://doi.org/10.1515/phys-2024-0014
received February 13, 2024; accepted March 25, 2024

Abstract: A binary blend of rosuvastatin (ROS) and teneligliptin (TEN) used for the management of cardiovascular complications require a simple, analytical process for the quality assurance of this formulation. UV absorption spectra of ROS and TEN showed overlapping spectra. Hence, the overlapped spectra of ROS and TEN were separated by ratio difference, ratio first derivative; constant extraction coupled with exponentiation with division spectrum, and induced dual-wavelength methods. The proposed methods were authenticated by following the international council for harmonization criteria. A good linear relationship was demonstrated by all four methods, in 2–15 and 2–30 µg/mL for ROS and TEN, respectively. The high percentage retrieval of 98.96–100.22 and 98.72–99.73% for ROS and TEN, respectively, with small relative error, assured the correctness of the techniques. The validated techniques were employed for concurrent evaluation of ROS and TEN from binary formulation and laboratory-prepared mixture. The standard addition process verified the reliability of the projected procedures. The developed methods showed same accuracy and precision when compared to the HPLC methods along with safer solvent. Finally, the environmental sustainability of the presented UV spectroscopic procedures was found to be better than the reported HPLC method. Hence, eco-friendly, simple, and accurate mathematically processed UV spectroscopic procedures can be employed for simultaneous quantification of ROS and TEN for routine quality control study.

Keywords: antidiabetic, rosuvastatin, teneligliptin, eco-friendly, ratio derivative spectroscopy

1 Introduction

Atherosclerosis and diabetes are major global health problems leading to many cardiovascular complications and are more common in obese patients. The risk of cardiovascular disease (CVD) is high in diabetics compared to non-diabetics due to additional health problems such as hypertension, dyslipidemia, *etc*. [1]. More than 500 million adults are suffering from diabetes and it is expected to rise to more than 750 million by 2045 [2,3]. The more common type is type 2 diabetes mellitus seen in adults and senior citizens. However, due to stress, lack of exercise, and environmental conditions, many teen agers are developing type 2 diabetes mellitus [4]. Many reports showed that patients with long time hyperglycemia are susceptible to atherosclerosis [1]. Atherosclerosis is a type of coronary artery disease caused by the accumulation of low-density lipoprotein on the artery's interior wall, making it narrow with loss of elasticity, along with the development of fatty veins and inflammation. The major difficulties of CVD are angina, myocardial infraction, and impulsive cardiac arrest [5–7]. Several statins are developed for lowering the total and low-density cholesterol in the blood and are the best choice for preventing atherosclerosis. However, the use of statins for long period leads to the development of diabetes [8]. Hence, maintaining a safer lipid profile and glycemic control is necessary to avoid health complications. An oral solid dosage formulation consisting of statin and gliptin is better for patients suffering from diabetes mellitus type -2 and dyslipidemia [9]. Teneligliptin (TEN, Figure 1a) is a third-generation oral antidiabetic drug acts by elevating the

* **Corresponding author: Mahesh Attimarad,** Department of Pharmaceutical Sciences, College of Clinical Pharmacy, King Faisal University, Al-Ahsa, Saudi Arabia, e-mail: mattimarad@kfu.edu.sa, tel: +966-553269799
Katharigatta Narayanaswamy Venugopala: Department of Pharmaceutical Sciences, College of Clinical Pharmacy, King Faisal University, Al-Ahsa, Saudi Arabia; Department of Biotechnology and Food Technology, Durban University of Technology, Durban, South Africa
Anroop B. Nair, **Bandar Aldhubiab**, **Sreeharsha Nagaraja:** Department of Pharmaceutical Sciences, College of Clinical Pharmacy, King Faisal University, Al-Ahsa, Saudi Arabia

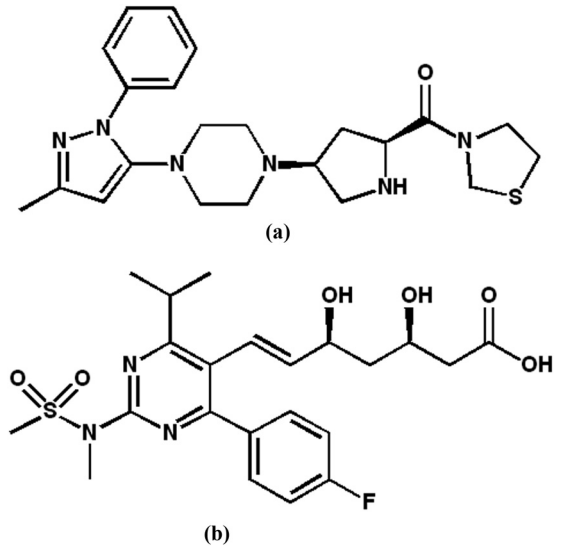

Figure 1: Chemical structure of TEN (a) and ROS (b).

level of incretin hormones by inhibiting the incretin hormone metabolizing enzyme dipeptidyl peptidase-4 enzyme. Thereby, increasing the insulin concentration and decreasing the glucagon amount in the blood, which also prolongs the retention of food in the stomach along with reducing the blood glucose level without hypoglycemic effect and weight gain [10–12].

Rosuvastatin (ROS, Figure 1b) is a new generation laboratory synthesized selective and irreversible blocker of enzyme 3-hydroxy-3-methylglutaryl coenzyme A (HMG-CoA) reductase. It obstructs the production of endogenous hepatic cholesterol, and the oxidation of LDL, which increases the reuptake of hepatic LDL from the blood. It also reduces the secretion of triglycerides by decreasing the formation of ApoB, and hence, is the first choice for the management of atherosclerosis [13,14].

A multicomponent formulation of ROS and TEN was used for the treatment of cardiovascular complications developed owing to elevated blood glucose concentration and high cholesterol levels. This combination showed better glycemic control and lipid profile with improved tolerability by the patients. A straightforward, environmentally safe analytical technique is desperately needed for this formulation's quality control. The quantification of ROS [15] and TEN along with other analytes were reported in the literature. ROS has been determined by spectrophotometric [16–19], spectrofluorometric [20], high performance thin layer chromatography [21], ultra-performance liquid chromatography (UPLC) [22,23], RP-HPLC [24–26], and liquid chromatography-mass spectrometry (LCMS) [27] in formulations and plasma samples single and with additional cardiovascular agents. Analysis of TEN alone and with metformin was achieved by spectrophotometry [28,29], reverse phase high performance liquid chromatography [30,31], UPLC [32], and LCMS [33] in formulations and biological samples. Few evaluation procedures are reported for the concurrent estimation of ROS and TEN from the binary preparation [34–36]. However, the documented procedures used hazardous substances such as buffers, acetonitrile, and methanol. Furthermore, HPLC method generates a high quantity of toxic waste owing to the prolonged elution time. Hence, to protect the environment, safer, simpler spectrophotometric approaches were established for the concurrent evaluation of ROS and TEN in pure, binary preparation and laboratory-prepared solution. The established methods involve the use of safe solvent ethanol and the separation of overlapped UV spectra by mathematical manipulation of saved spectra with minimum waste formation. Finally, the greenness of the established approaches were compared with the documented HPLC procedure using Raynie *et al.* green analytical procedure index (GAPI), and Analytical GREEnness Metric (AGREE) tools.

2 Experimental methods

2.1 Materials and reagents

Pure standards of ROS and TEN with certified purity of 99.8 and 99.7%, respectively, were picked up from Biokemix Ltd (Hyderabad, India). Pure Ethanol (99.5%) and methanol (99.85%) were procured from Scharlau (Sentmenat, Spain). A formulation consisting of ROS (10.0 mg) and TEN (20.0 mg) was acquired from the Indian local pharmacy.

2.2 Apparatus and software

A UV-Vis spectrophotometer (1600 Shimadzu, Japan) connected to a desktop mounted with UV-probe (Shimadzu, Ver 2.2) was used to record the UV absorption spectra. Matching quartz cuvettes (1 cm) were used for blank and analyte solutions. An ultrasonic bath sonicator (LeelaSonic 50, Thane, India) was used for the preparation of sample solutions.

2.3 Preparation of reliable standards

To arrange authentic solutions for 1.0 mg/mL of ROS and TEN, 100.0 mg of each analyte were separately added to a 100.0 mL graduated flask filled with methanol. The necessary amount of stock solution was adulterated with ethanol to create the working standard solutions of TEN and ROS (100.0 µg/mL).

2.4 Preparation of laboratory mixed solutions.

By carefully moving the working standard solutions of ROS and TEN into a sequence of 5.0 mL graduated flasks, diverse fractions of ROS and TEN solutions were arranged. The total quantity of the solution was adjusted with the ethanol to attain an ultimate amount of 5:10, 10:20, 15:30, 10:30, and 15:10 µg/mL of ROS and TEN respectively.

2.5 Preparation of tablet solution

Fixed-dose combination tablets with ROS (10.0 mg) and TEN (20.0 mg) label claims were weighed and crushed into fine powder. A sufficient amount of powder was placed in a 10.0 mL graduated flask containing 5.0 mL of methanol. The volumetric flask was sonicated for 15 min before being separated into a second volumetric flask. The remainder was rinsed and the ultimate capacity was attuned to the mark to get the sample solution comprising 10.0 mg/mL of ROS and 20.0 mg/mL of TEN. The concentration was reduced to the calibration range with ethanol before analysis. The conventional standard adding procedure was adopted to confirm the correctness of the approaches. A predetermined quantity of TEN and ROS were added to the formulation that had previously been examined, and the standard deviation and percentage recovery of the added amount were examined.

2.6 Calibration curves

The zero-order absorption spectra (^{0}D) were documented between 200 and 400 nm independently for ROS and TEN using a series of a solution having a concentration of 2.0–15.0 and 2.0–30.0 µg/mL, respectively. Similarly, the seven different solutions of a combination of analytes falling within the previously mentioned concentration range were organized, and UV absorption spectra were captured and digitally preserved.

2.6.1 Ratio difference spectroscopic (RDS) method

The ^{0}D spectra of ROS (2.0–15.0 µg/mL) after division by the spectrum of TEN (5.0 µg/mL) created ratio-spectra, which were smoothened with 4 nm. A linear relationship was created by drawing the crest height dissimilarity among 307.8 nm and 259.9 nm against the respective amount of ROS. Correspondingly, the spectrum of ROS (2.0 µg/mL) was used to divide the TEN (2.0–30.0 µg/mL) spectra. The peak intensity variance among 256.9 nm and 295.0 nm from the ratio spectra was graphed in contrast to the respective quantity of TEN to create the linear relationship and correlation equation.

2.6.2 Ratio first-derivative spectroscopic (RFS) method

The ratio spectra of TEN and ROS have been turned toward ratio first-order derivative spectra using an increment of 10 and a 2 nm as Δλ. Peak amplitude measurements have been obtained at 297.6 nm and 215.2 nm, respectively, for ROS (2.0–15.0 µg/mL) and TEN (2.0–30.0 µg/mL). The direct relationship was computed between peak heights and respective concentrations.

2.6.3 Constant extraction coupled with multiplication (CEM) with divisor spectra method

Calibration curves were established by measuring the absorbance of ^{0}D spectra of ROS (2.0–15.0 µg/mL) and TEN (2.0–30.0 µg/mL) at 242.9 nm and 245.7 nm, respectively, against corresponding concentrations of ROS and TEN.

2.6.4 Induced dual wavelength (IDW) method

A calibration curve for ROS (2.0–15.0 µg/mL) was created by assessing the absorbance at 306 nm compared to the corresponding concertation. For TEN the absorbance was determined by subtracting the product of absorbance at 301.0 nm and 3.638 from the absorbance at 245.7 nm of the mixture spectra having a series of TEN concentration (2.0–30.0 µg/mL). Then, the calibration curve and correlation equations were computed from the absorbance and corresponding concentrations.

3 Results and discussion

Because it is easy to use, quick, accurate, and repeatable, the UV spectrophotometric method of analysis has been widely utilized for consistent quality assurance of tablets. Nevertheless, most of the potent medicines are small heterocyclic/aromatic compounds with good UV absorption. Hence, multicomponent formulation shows ample overlap

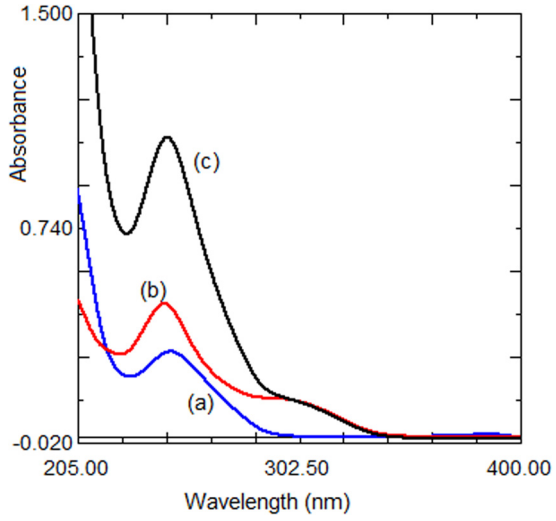

Figure 2: UV spectra of (a) TEN, (b) ROS, and (c) combination.

of UV absorption spectra, making it challenging to quantify simultaneously without separation. UV absorption spectra of ROS and TEN showed overlapping spectra (Figure 2); however, TEN has no absorption above 300.0 nm allowing quantification of ROS but preventing analysis of TEN in the presence of ROS. Hence, different mathematically processed *in silico* UV spectroscopic methods were established [37–41].

ROS calcium (pKa 4.76, LogP 1.92) is soluble in acetonitrile and methanol; however, it is sparingly soluble in water and ethanol. TEN (pKa 8.78, LogP 1.5) completely dissolve in water, methanol, faintly soluble in ethanol, and insoluble in acetonitrile. Hence, for dissolving both the analytes, methanol was used and further dilution was made with ethanol.

Analysis of multicomponent formulations by spectrophotometric methods is challenging for the analytes showing overlapped spectra. Several spectral resolution techniques are developed for the simultaneous determination of such multicomponent formulations [37–41].

3.1 RDS method

In the present work, the RDS method was utilized to separate the overlapped spectra of ROS and TEN by converting the parent UV absorption spectra of ROS (2.0–15.0 µg/mL) and TEN (2.0–30.0 µg/mL) to ratio spectra by apportioning with TEN (5.0 µg/mL) and ROS (2.0 µg/mL) correspondingly (Figure 3a and b). Different concentrations of TEN and ROS were envisaged to select the appropriate concentration to get reproducible ratio spectra. With a high concentration spectrum as a divisor, a low peak amplitude with less noise was observed. However, with low concentration, the noise was high but a good amplitude was obtained. Nevertheless, to generate noiseless ratio spectra, spectra were equalized using 4 nm. The ratio spectra of the bi-component appear above the zero line and the ratio spectra of the pure analyte. The amplitude of the difference between the apex and the valley, however, was the same. The two wavelengths selected were the crest and valley of the ratio spectra and the difference is directly proportionate to the amount of the analytes. The wavelengths 307.8 and 259.9 nm for ROS and 256.9 and 295.0 nm for TEN were selected and the linearity graph was created in contrast to the equivalent amount of analytes. Further, a similar peak amplitude difference was observed for pure and mixture ratio spectra having the equal amount of ROS and TEN (Figure 3c and d).

3.2 RFS method

Derivative UV spectrophotometry has been extensively used for the simultaneous quantification of multicomponent formulations due to its resolution capacity of the overlapped spectra along with the improvement of spectral specificity. Derivatization of UV spectra has high-resolution power and is easy due to available simple computer software [37–41].

In this project, to remove the influence on the second analyte (constant K = zero), the ratio spectra have been altered into first-order derivative spectra. Further, derivative spectra offer several maxima and minima, which progressively increase with the increase in the concentration of the analytes and hence could be used for quantification of analytes without interference from the other analytes. Series of 2, 4, and 8 nm were envisaged as $\Delta\lambda$ for differentiation and 4 nm exhibited smooth first derivative spectra. Using a scaling increment of 10, the apex height was raised. The first-order derivatization of spectra of ROS depicted several maxima and minima (Figure 4a). The peak height at 297.6 nm was superior along with tremendous reproducibility. Henceforward, 297.6 nm was selected for the building of the linearity curve. Likewise, 1D spectra of TEN showed several maxima and minima with better peak amplitude at 215.2 and 281.7 nm (Figure 4b). However, the sensitivity and reproducibility were better at 215.2 nm and hence selected for the building of the linearity curve. Further, similar apex height was observed for pure and mixture ^{1}D spectra having the same quantity of ROS and TEN at 297.6 and 215.2 nm, respectively (Figure 4c and d).

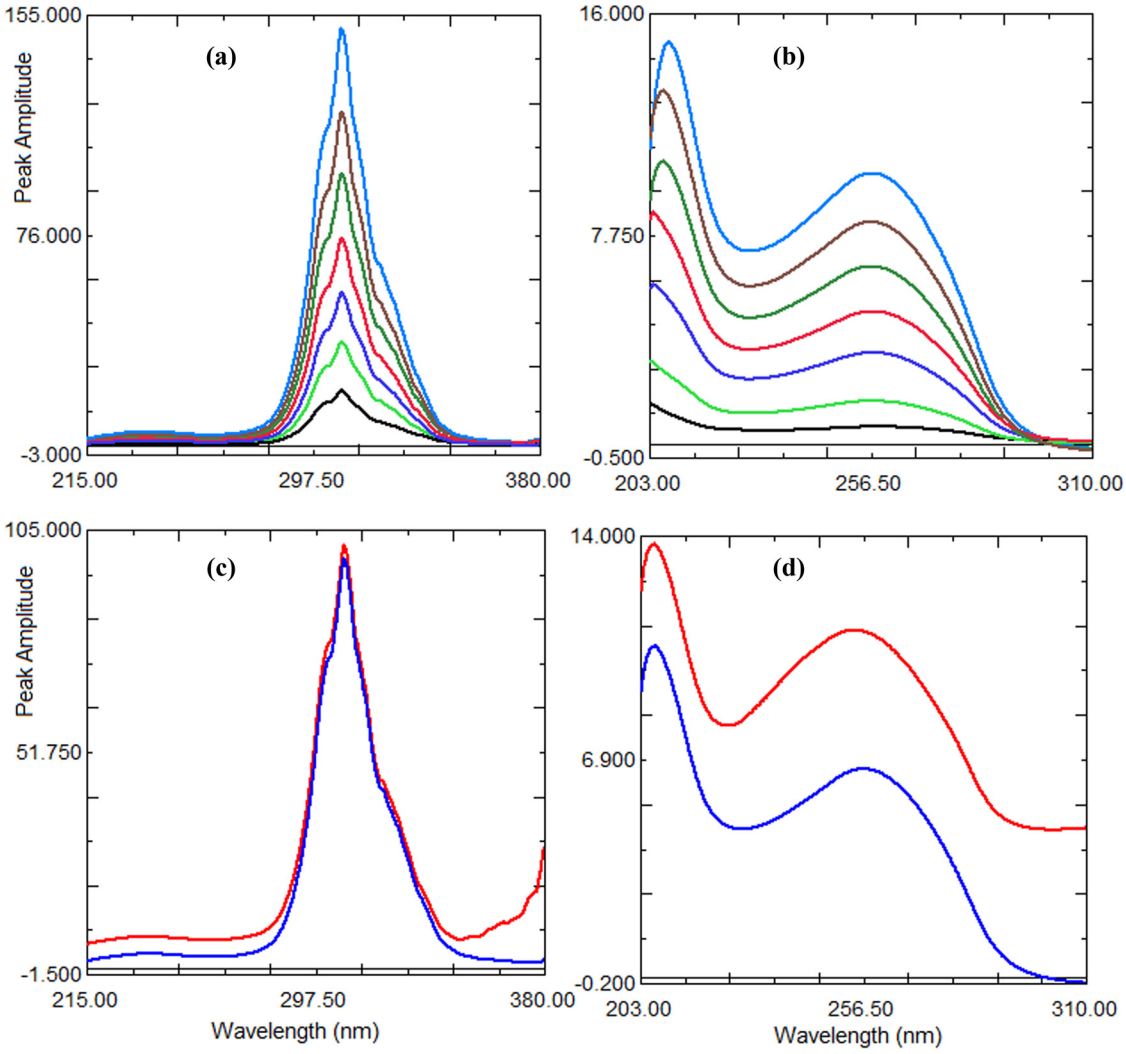

Figure 3: Ratio spectra of ROS (2.0–15.0 µg/mL) by TEN spectrum (5.0 µg/mL) as denominator (a). Ratio spectra of TEN (2.0–30.0 µg/mL) with ROS spectrum (2.0 µg/mL) as denominator (b). Comparison between ratio spectra generated from pure ROS (c) and TEN (d) and from mixture (Red).

3.3 CEM with divisor spectra method

Constant extraction starts with the determination of constant for bi-component ratio spectra using the linear regression equation generated using ratio spectra of the pure analyte, coupled with the multiplication of this constant by divisor spectrum for isolation of zero order spectra. This method involves the isolation of ^{0}D spectra of individual components from the bi-component spectrum. It was accomplished by taking the constant out of the ratio spectra and multiplying the resultant ratio spectrum by the divisor spectrum. In the present work, for quantification of ROS and TEN from the bi-component mixture, ratio spectra of pure ROS and TEN were created by apportioning the sequence of ROS and TEN spectra by TEN (5.0 µg/mL) and ROS (2.0 µg/mL) spectra, respectively. The linear correlation was established among peak height variance (ΔQ) at 307.8 and 259.9 nm in contrast to postulated crest amplitude (Q_{pos}) at 307.8 nm for ROS. The linear curve for ROS and TEN was ΔQ_R (307.8–259.9) = 0.9729 ROS/TEN' + 0.0709 (R^2 = 1.000) and ΔQ_T (256.9–295.0) = 0.9972 TEN/ROS' + 0.1877. (R^2 = 0.9994), respectively.

For quantification of ROS, divisor spectra of ROS (2.0 µg/mL) were utilized. Using the ratio spectra of pure TEN/ROS', a direct relationship was constructed amongst the peak amplitude difference (Q 256.9–295.0 nm) and postulated peak amplitude (Q_{pos}) at 256.9 nm. Then, the recorded apex height from the mixture's ratio spectra represented by means of TEN/ROS' + ROS/ROS'. By deducting the hypothesized apex elevation at 256.9 nm from the observed apex height, the constant value (ROS/ROS') was calculated. Next multiplying this constant by the divisor spectra of ROS' yielded the zero-order spectra of ROS

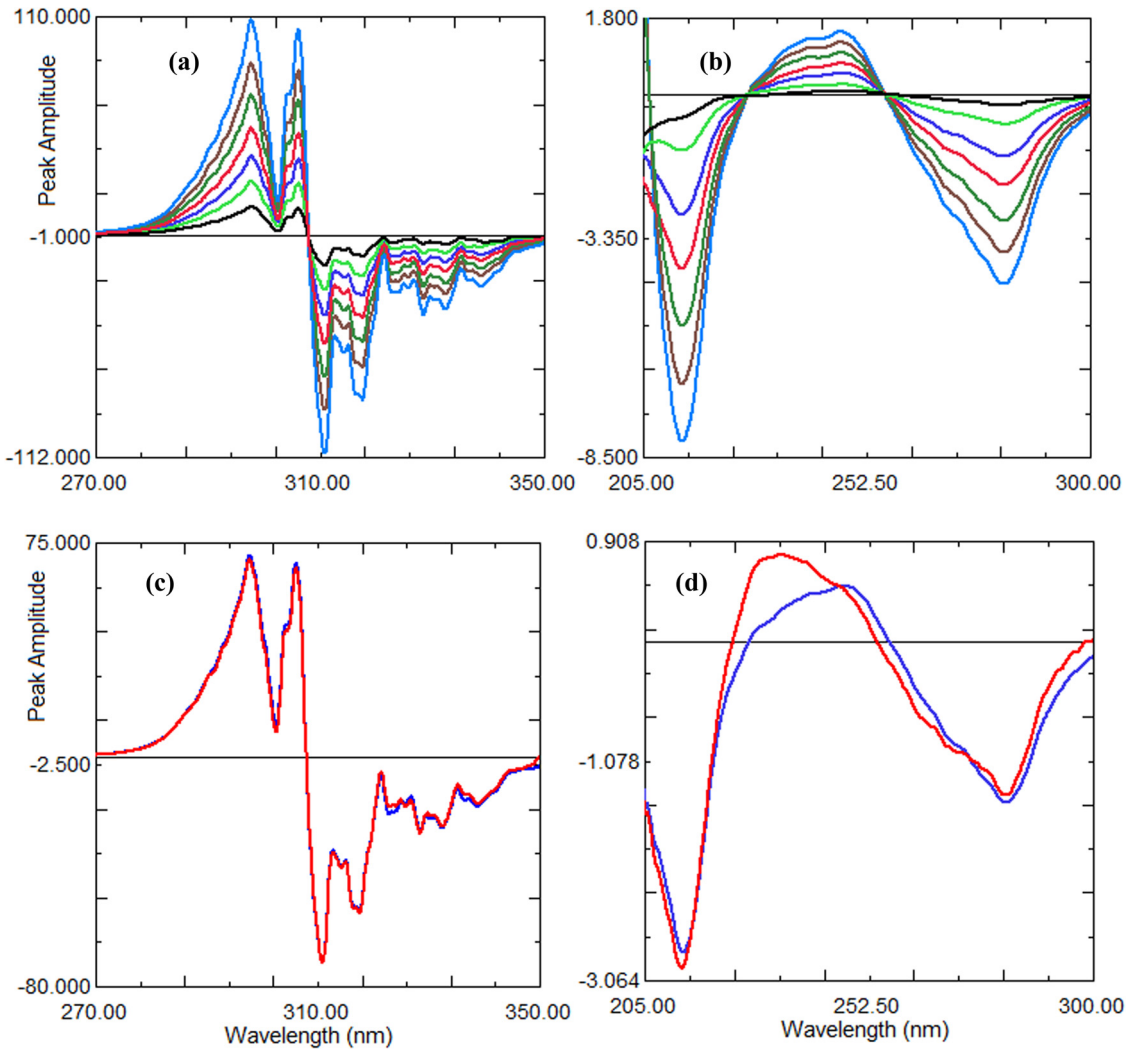

Figure 4: (a) Ratio ^{1}D spectra of ROS (2.0–15.0 µg/mL) with TEN spectrum (5.0 µg/mL) as denominator. (b) Ratio ^{1}D spectra of TEN (2.0–30.0 µg/mL) with ROS spectrum (2.0 µg/mL) as denominator. Comparison between ^{1}D ratio spectra generated from (c) pure ROS and (d) TEN and (Red) from mixture.

(Figure 5a). By measuring the absorbance at the mixture's λ_{max} (256.9 nm) and using a regression equation produced from the calibration curve developed using zero-order spectra of pure ROS in the series of 2.0–15.0 µg/mL at 256.9 nm, the concentration of ROS in the mixture was ascertained.

Similarly, for quantification of TEN from the binary mixture, a ratio spectrum ROS/TEN' + TEN/TEN' was obtained by dividing the mixture spectrum with the TEN spectrum, and the recorded peak height (Q_{Rec}) was calculated at 307.8 nm. The constant TEN/TEN' was obtained by removing the hypothesized apex height (Q_{pos}) from the recorded apex height (Q_{Rec}) at 307.8 nm. The product of factor and the denominator spectrum (TNE') yielded the ^{0}D spectra on TEN present in the mixture (Figure 5b). The amount of TEN was computed by quantifying the absorbance at its λ_{max} (245.7 nm) and regression equation generated from the calibration curve developed using ^{0}D spectra of pure TEN in the series of 2.0–30.0 µg/mL at 245.7 nm.

3.4 IDW method

In the present work, this technique was utilized for the assessment of TEN as TEN was completely overlapped by the spectrum of ROS. Whereas, ROS showed an extended peak above 300.0 nm where TEN had no absorption. Hence, a wavelength of 306.0 nm was selected to determine ROS, ROS showed good reproducibility and sensitivity without any interference from the TEN as shown in (Figure 2) at 306.0 nm, hence direct relationship was computed by measuring absorption at 306.0 nm against respective

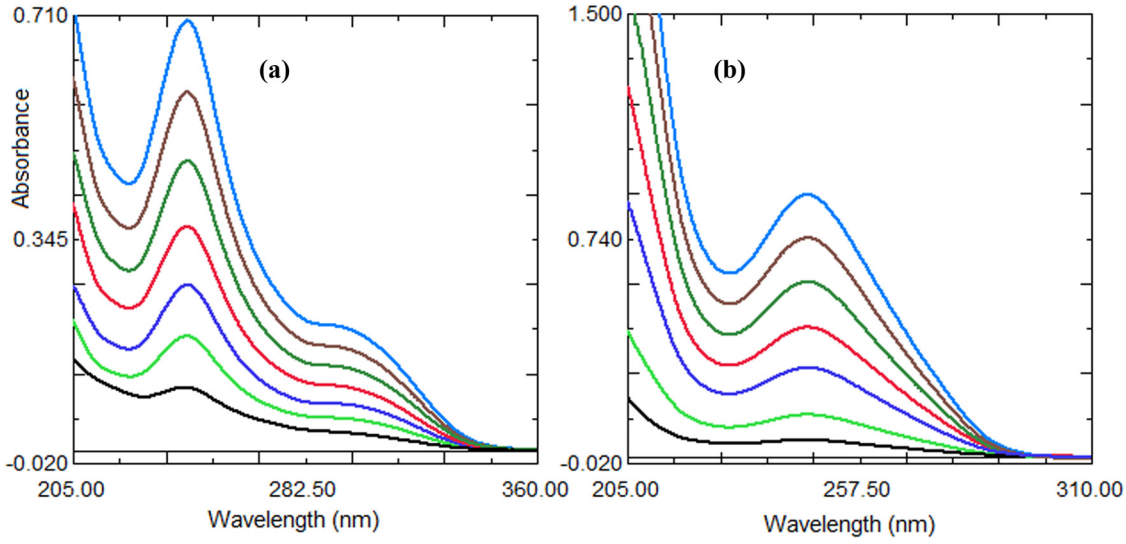

Figure 5: Zero-order absorption spectra of (a) ROS (2.0–15.0 µg/mL), and (b) TEN (2.0–30.0 µg/mL).

concentration. ROS showed overlapping at λ_{max} wavelength of TEN (245.7 nm), hence absorption factor for ROS was determined at selected two wavelengths to eliminate the interference by ROS at λ_{max} wavelength of TEN. The pair of wavelengths chosen were 245.7 and 301.0 nm and the absorption of TEN was determined from the mixture spectra using Eq. (1)

$$A_{\text{TEN}\cdot 245.7\ \text{nm}} = A_{\text{RT}\cdot 245.7\ \text{nm}} - (A_{\lambda 1}/A_{\lambda 2}) \times A_{\text{RT}\cdot 301.0\ \text{nm}}, \quad (1)$$

where A_{RT} represents the absorption of mixture ratio spectra, and $A_{\lambda 1}/A_{\lambda 2}$ is the absorption factor of ROS at 245.7 and 301.0 nm, respectively. A linearity curve was created for ROS and TEN by calculating the absorption at 306.0 and 245.7 nm, respectively against corresponding concentrations. Quantification of ROS from the mixture was computed by determining the absorption at 306.0 nm and the corresponding linearity equation. For quantification of TEN from the mixture, absorption was calculated at 245.7 nm by using the above equation and concentration was computed from the respective regression equation. The absorption factor was calculated using three different concentrations of ROS in the calibration range and was found to be 3.638.

3.5 Validation of analytical method and statistical analysis

Using the international council for harmonization guidelines, validation constraints including linearity, limits of detection (LOD), limits of quantification (LOQ), accuracy, precision, and specificity were verified to determine whether the suggested analytical procedures were applicable for the quality control of ROS and TEN formulations.

3.5.1 Linearity

A series of seven concentrations in the series of 2.0–15.0 and 2.0–30.0 µg/mL of ROS and TEN, respectively, were evaluated for the construction of a calibration curve. Both the analytes exhibited good linearity in the above-mentioned concentrations in all four methods with excellent coefficient of determination ($R^2 > 0.998$).

3.5.2 Sensitivity

To demonstrate the sensitivity of the procedure, the LOQ and LOD were employed. The formulas for calculating LOD and LOQ were 3.3 SD/slope and 10*SD/slope, where SD is the standard deviation of the response. The determined LOD and LOQ are tabulated in Table 1.

3.5.3 Accuracy

Accuracy was confirmed by performing the analysis of three diverse amounts of both components in the linearity range. Accuracy was articulated as percentage recovery and percentage relative error. Percentage recovery (Table 1) was found to be 98.96–100.22 and 98.72–99.73% for ROS and TEN, respectively. The low relative percentage error

Table 1: Validation outcomes of ROS and TEN by anticipated UV-spectrophotometric procedures

	RDS		RFS		CEM		IDW	
Parameters	**ROS**	**TEN**	**ROS**	**TEN**	**ROS**	**TEN**	**ROS**	**TEN**
Linearity								
Wavelength (nm)	307.8–259.5	256.9–295.0	297.6	215.2	242.9	245.7	306.0	245.7
Linearity range (μg/mL)	2–15	2–30	2–15	2–30	2–15	2–30	2–15	2–30
Slope	9.8496	0.3276	7.1725	0.2523	0.0471	0.0294	0.0126	0.0302
Intercept	−3.602	−0.1871	−2.207	−0.044	+0.0021	+0.0029	+0.0029	−0.0133
Coefficient of determination (R^2)	0.9997	0.9996	0.9999	0.9998	0.9997	0.9998	0.9998	0.9999
Sensitivity								
LOD (μg/mL)	0.039	0.128	0.173	0.129	0.294	0.503	0.231	0.300
LOQ (μg/mL)	0.118	0.388	0.525	0.392	0.891	1.526	0.701	0.911
Accuracy (mean % recovery ± % relative error)								
Within day	99.09 ± 0.91	99.73 ± 0.27	100.22 ± 0.22	98.72 ± 1.28	99.56 ± 0.44	99.07 ± 0.93	99.80 ± 0.20	99.26 ± 0.74
Between day	98.96 ± 1.04	99.63 ± 0.37	99.07 ± 0.93	99.20 ± 0.80	99.62 ± 0.38	98.78 ± 1.22	100.09 ± 0.09	99.52 ± 0.48
Precision (mean % relative standard deviation [RSD])								
Within day	1.30	0.97	1.42	1.11	1.40	1.68	1.40	1.37
Between Day	1.44	1.45	1.43	0.93	1.87	1.88	1.29	1.38
Robustness study by wavelength (±2 nm) (%RSD)								
Wavelength (+2 nm)	0.89	1.08	1.94	1.23	0.92	0.87	0.85	1.15
Wavelength (−2 nm)	1.24	1.38	0.86	1.62	1.73	0.95	1.19	1.75

Acceptable % RE: ± 2%; %RSD: ± 2%; % recovery: 98.00–102.00%.

(Table 1) further confirmed the accurateness of the projected procedures.

3.5.4 Precision

The overhead-arranged solutions were investigated on the first day to appreciate the intraday/repeatability of the methods. To find the interday/intermediate precision, the same solutions were examined 3 days in a row. Table 1 demonstrates that the precision was confirmed for both analytes, with the percentage relative standard deviation for each technique being less than 2.

3.5.5 Specificity

The diverse ratio of ROS and TEN close to the ratio of the formulation was prepared based on the formulation concentration in addition to some ratios with little higher and lower amount and evaluated by the anticipated procedures to ascertain the specificity of the method. The percentage recovery was close to the actual concentrations of both analytes, along with a low standard deviation (Table 2).

3.5.6 Robustness study

The robustness of the suggested UV-spectroscopic methods was evaluated by varying the wavelength by ±2 nm and evaluating a mixture of 10 and 20 μg/mL of ROS and TEN, respectively. The assay results were used to compute the % RSD. With just minor modifications to the experimental circumstances, the proposed approach remains stable, as seen by the %RSD values falling within the acceptable range of ±2% (Table 1).

3.6 Analysis of pharmaceutical formulation

The presented UV spectroscopic procedures were successfully applied to the fixed combination of ROS and TEN. The analysis results of the simultaneous determination of both analytes are in agreement with the quantity of the components in the formulation (Table 3). The conventional addition method verified the validity of the methods. The percentage recovery of the extra quantities of both analytes ranged from 98.00 to 102.00% with an almost insignificant standard deviation. Furthermore, a statistical comparison was made utilizing the student's *t*-test and *F*

Table 2: Evaluation outcomes of laboratory-prepared solutions by anticipated UV-spectrophotometric procedures

Ratios[a]	RDS (% recovory ± SD)		RFS (% recovory ± SD)		CEM (% recovory ± SD)		IDW (% recovory ± SD)	
ROS: TEN	ROS	TEN	ROS	TEN	ROS	TEN	ROS	TEN
5:10	99.34 ± 0.87	100.16 ± 1.32	100.74 ± 0.35	99.82 ± 1.24	99.75 ± 1.01	99.69 ± 1.36	99.76 ± 0.99	99.76 ± 1.07
10:20	99.78 ± 1.51	99.48 ± 1.42	100.17 ± 0.79	99.65 ± 0.95	99.78 ± 1.02	99.67 ± 0.77	99.65 ± 1.05	100.16 ± 0.72
15:30	100.02 ± 1.52	100.3 ± 1.00	100.06 ± 1.46	99.53 ± 0.88	99.14 ± 0.62	100.51 ± 0.74	99.66 ± 0.76	99.19 ± 0.68
10:30	99.59 ± 1.01	99.87 ± 0.71	100.12 ± 1.45	99.82 ± 1.48	98.91 ± 0.3	99.76 ± 1.33	99.62 ± 0.84	98.87 ± 0.59
15:10	99.64 ± 1.58	101.08 ± 0.75	99.23 ± 1.62	99.49 ± 0.63	100.4 ± 0.64	99.38 ± 1.05	99.99 ± 0.82	99.34 ± 1.15

[a]ratios in µg/mL; SD: Standard deviation; Acceptable % RSD: ± 2%; % recovery: 98.00–102.00%.

Table 3: Analysis results of binary blend of ROS and TEN and statistical comparison with HPLC method

	RDS		RFS		CEM		IDW		Reported HPLC method [34]	
Parameters	ROS	TEN	ROS	TEN	ROS	TEN	ROS	TEN	ROS	TEN
Label claim[a]	10	20	10	20	10	20	10	20	10	20
Amount taken[b]	5	10	5	10	5	10	5	10	5	10
Amount found[bc] ± SD	4.96 ± 0.05	9.92 ± 0.08	4.96 ± 0.09	9.93 ± 0.24	4.94 ± 0.05	10.04 ± 0.17	4.93 ± 0.04	9.96 ± 0.11	5.02 ± 0.06	9.86 ± 0.04
% Labeled claim	100.21	99.92	100.28	99.58	99.57	99.51	99.03	99.01	99.72	99.53
Statistical analysis										
n	6	6	6	6	6	6	6	6	—	—
Students *t*-test[d]	0.803	0.37	0.92	0.27	0.07	0.06	1.08	1.11	—	—
F[e]	1.04	2.07	1.03	2.02	1.38	1.57	1.61	1.42	—	—

[a]mg/tablet, [b]µg/mL, [c]Average of six repetitions made at every level; SD: Standard deviation, critical value for students *t*-test: 2.228([d]) and *F* test: 5.050([e]).
HPLC: Zorbax C_{18} column (150 × 4.6 mm) 5 µm, Mobile phase: Phosphate buffer (pH 3.5) and methanol: 70:30% (v/v), flow rate 1 mL/min, at 240 nm.

test between the outcomes and the reported HPLC method [34]. For the suggested methods, the computed *F* and *t* values were below the critical values, indicating no significant dissimilarity in the assessed outcomes between the presented UV methods and described the HPLC process in terms of accuracy and precision (Table 4).

3.7 Assessment and comparison of greenness with reported HPLC method

The greenness of the developed UV spectroscopic methods were evaluated using three different tools and compared with the reported HPLC method [34]. The first greenness method was based on semi quantitative method reported by Raynie and Driver [42] represented by pentagon with five parameters: health, safety, environment, energy, and waste generated (Figure 6a and b). The proposed UV spectroscopic methods are green analytical methods because the solvent used is ethanol which is safer when compared to other UV and HPLC methods, which utilized methanol and acetonitrile as solvents. Further, comparing this to HPLC procedures reveals even lower waste generation and energy use, hence the developed UV-spectroscopic methods are environment friendly.

In the second greenness tool, GAPI, evaluates 15 different parameters including the sample collection, transport, storage, preparation, type of method, safety of solvents, amount of reagents, energy utilized, waste generated, and its treatment and occupational hazards with additional mark for quantitative procedure [43]. The generated pictograms (Figure 6c and d) upon examination visually demonstrated the positive features of spectrophotometry processes over HPLC method. The solvents used in the UV spectroscopic method is ethanol, hence it is safer. GAPI evaluation also confirmed that the amount of solvent used, health safety hazard, and energy required are in favor of UV spectroscopic method compared to HPLC method. Another advantage for the spectrophotometry approach

Table 4: Standard adding technique results of binary blend of ROS and TEN

Amount added (µg/mL)		ROS (Mean % recovery)				TEN (Mean % recovery)			
ROS	**TEN**	**RDS**	**RFS**	**CEM**	**IDW**	**RDS**	**RFS**	**CEM**	**IDW**
2.5	5	100.45	100.62	98.48	99.63	98.76	100.54	100.67	101.34
5	10	100.57	100.86	98.37	98.83	98.81	99.07	100.44	100.62
7.5	15	99.06	100.92	100.65	100.75	100.83	101.73	100.03	99.54
Across mean		100.03	100.80	99.17	99.74	99.47	100.45	100.38	100.50
%RSD		0.84	0.16	1.30	0.97	1.19	1.33	0.32	0.90

% RSD: Percent relative standard deviation; acceptable % RSD: ± 2%; % recovery: 98.00–102.00%.

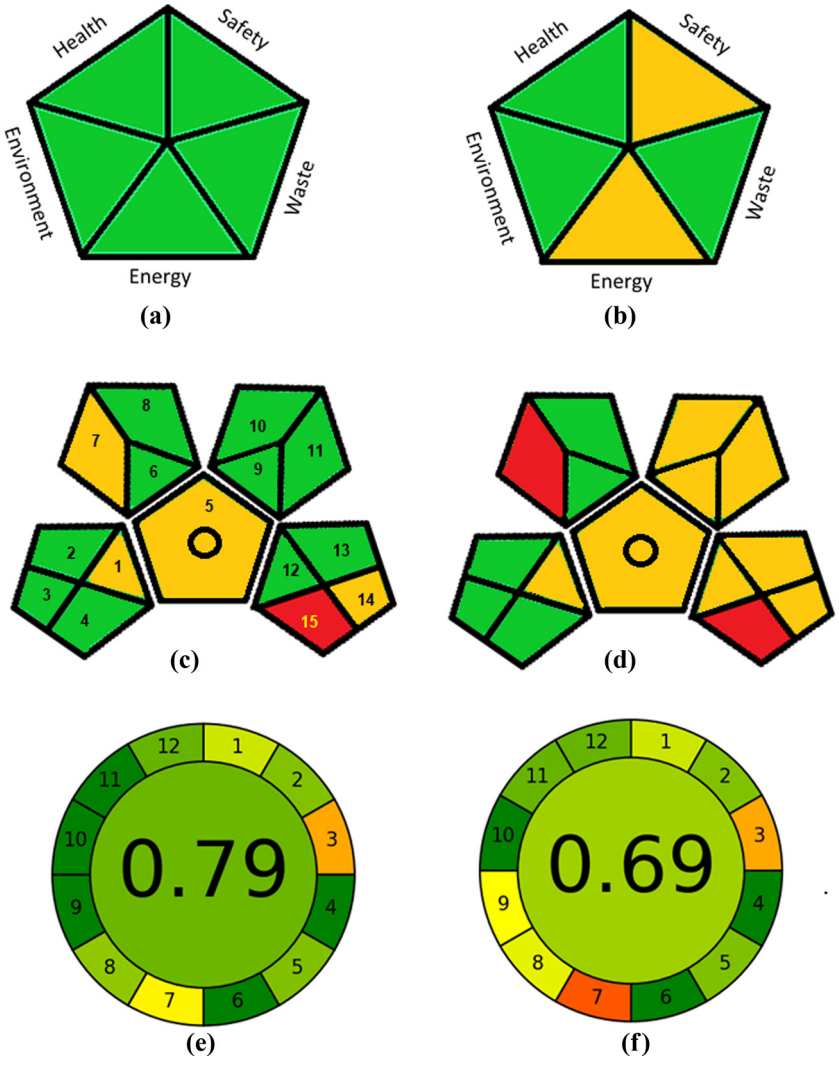

Figure 6: Greenness results of UV spectroscopic (a), (c), and (e); HPLC (b), (d), and (f); techniques by Raynie *et al.* (a) and (b); GAPI (c) and (d); and AGREE (e) and (f).

comes from the fact that the amount of waste generated per sample by the HPLC-UV is more than 10 mL. AGREE is a quantitative greenness evaluation tool based on the 12 principles of green analytical chemistry [44]. Software generates the greenness findings, which are displayed as a circle with an overall score at the center and the

contributions of 12 principles around the circle's circumference. (Figure 6e and f). The suggested UV spectroscopic approaches had more green segments and a higher total score of 0.79 compared to 0.69 for the HPLC method, confirming the environment friendly nature of the proposed UV spectroscopic methods.

4 Conclusion

The presented mathematically modified UV spectrophotometric techniques are simple, accurate, and reproducible for concurrent determination of ROS and TEN from binary formulation devoid of any preliminary separation and without interference from the formulation adjuvants. Further, the manipulation was performed using the software provided with the instrument and involves fewer steps. The CEM method was used to extract the ^{0}D spectra of analytes from the combination and quantification was performed at λ_{max} wavelength, a fingerprint of the analytes. The developed methods use an ecofriendly nature solvent system with less generation of waste compared to the HPLC methods, making the methods green. Further, the statistical comparison of assay results confirmed that no discernible discrepancies was detected in relation to correctness and precision between the projected UV spectroscopic and the documented HPLC procedure. As a result, the environmentally friendly spectroscopic techniques that have been presented may be used in pharmaceutical companies, research, and drug-testing labs to control the quality of ROS and TEN formulations, as these methods have fewer sample preparation steps and fast analysis time compared to the HPLC techniques.

Acknowledgments: The authors are thankful to the Deanship of Scientific Research, Vice Presidency for Graduate Studies and Scientific Research, King Faisal University, Al-Ahsa, Saudi Arabia for the support.

Funding information: This work was supported by the Deanship of Scientific Research, Vice Presidency for Graduate Studies and Scientific Research, King Faisal University, Saudi Arabia (GRANT6026).

Author contributions: All authors have accepted responsibility for the entire content of this manuscript and approved its submission.

Conflict of interest: The authors state no conflict of interest.

Data availability statement: All data generated or analyzed during this study are included in this published article.

References

[1] Poznyak A, Grechko AV, Poggio P, Myasoedova VA, Alfieri V, Orekhov AN. The diabetes mellitus-atherosclerosis connection: the role of lipid and glucose metabolism and chronic inflammation. Int J Mol Sci. 2020;21(5):1835. doi: 10.3390/ijms21051835.

[2] International Diabetes Federation. IDF Diabetes Atlas. 10th edn. Brussels, Belgium; 2021. https://www.diabetesatlas.org.

[3] Mayer-Davis EJ, Lawrence JM, Dabelea D, Divers J, Isom S, Dolan L, et al. Search for diabetes in youth study. Incidence trends of type 1 and type 2 diabetes among youths 2002–2012. N Engl J Med. 2017;376:1419–29. doi: 10.1056/NEJMoa1610187. pmid:28402773.

[4] Xie J, Wang M, Long Z, Ning H, Li J, Cao Y, et al. Global burden of type 2 diabetes in adolescents and young adults, 1990-2019: systematic analysis of the global burden of disease study 2019. BMJ. 2022;379:e072385. doi: 10.1136/bmj-2022-072385.

[5] Libby P, Buring JE, Badimon L, Hansson GK, Deanfield J, Bittencourt MS, et al. Atherosclerosis. Nat Rev Dis Primers. 2019;5:56. doi: 10.1038/s41572-019-0106-z.

[6] Kronenberg F, Mora S, Stroes ESG, Ference BA, Arsenault BJ, Berglund L, et al. Lipoprotein(a) in atherosclerotic cardiovascular disease and aortic stenosis: a European Atherosclerosis Society consensus statement. Eur Heart J. 2022;43(3):3925–46. doi: 10.1093/eurheartj/ehac361

[7] Tian W, Zhang T, Wang X, Zhang J, Ju J, Xu H. Global research trends in atherosclerosis: A bibliometric and visualized study. Front Cardiovasc Med. 2022;9:956482. doi: 10.3389/fcvm.2022.956482.

[8] Crandall JP, Mather K, Rajpathak SN. Statin use and risk of developing diabetes: results from the diabetes prevention program. BMJ Open Diabetes Res Care. 2017;5:e000438. doi: 10.1136/bmjdrc-2017-000438.

[9] Scheen AJ. Pharmacokinetic evaluation of atorvastatin and sitagliptin in combination for the treatment of type 2 diabetes. Expert Opin Drug Metab Toxico. 2012;8(6):745–58. doi: 10.1517/17425255.2012.686603.

[10] Li X, Huang X, Bai C, Qin D, Cao S, Mei Q, et al. Efficacy and safety of teneligliptin in patients with type 2 diabetes mellitus: A systematic review and meta-analysis of randomized controlled trials. Front Pharmacol. 2018;9:449. doi: 10.3389/fphar.2018.00449.

[11] Sharma SK, Panneerselvam A, Singh KP, Parmar G, Gadge P, Swami OC. Teneligliptin in management of type 2 diabetes mellitus. Diabetes Metab Syndr Obes. 2016;9:251–60. doi: 10.2147/DMSO.S106133.

[12] Kishimoto M. Teneligliptin: a DPP-4 inhibitor for the treatment of type 2 diabetes. Diabetes Metab Syndr Obes. 2013;6:187–95. doi: 10.2147/DMSO.S35682.

[13] Luvai A, Mbagaya W, Hall AS, Barth JH. Rosuvastatin: a review of the pharmacology and clinical effectiveness in cardiovascular disease. Clin Med Insights Cardiol. 2012;6:17–33. doi: 10.4137/CMC.S4324.

[14] Rosenson RS. Statins in atherosclerosis: lipid-lowering agents with antioxidant capabilities. Atherosclerosis. 2004;173(1):1–12. doi: 10.1016/S0021-9150(03)00239-9.

[15] Ângelo ML, Moreira FL, Morais RAL, Santos ALA, Salgado HRN, Araújo MBD. Analytical methods for the determination of rosuvastatin in pharmaceutical formulations and biological fluids: a critical review. Crit Rev Anal Chem. 2018;48(4):317–29. doi: 10.1080/10408347.2018.1439364.

[16] Halka L, Kucher T, Kryskiw L, Piponski M, Furdela I, Uglyar T, et al. Development of the spectrophotometric method for the determination of rosuvastatin in tablets by using bromophenol blue. Sci: Pharm Sci. 2023;2(42):11–9. doi: 10.15587/2519-4852.2023.277461.

[17] Lima M, Cassella R, Pacheco W. Spectrophotometric determination of rosuvastatin in pharmaceutical formulations using quinalizarin. Braz J Pharm Sci. 2017;53:1–8. doi: 10.1590/s2175-97902017000300075.

[18] Hegazy MA, Bakr MA, Badawey AM, Abbas SS. Univariate and multivariate assisted spectrophotometric methods for determination of rosuvastatin calcium and fenofibrate in bulk powders and tablets along with their degradation products. Spectrochim Acta A Mol Biomol Spectrosc. 2021;248(5):119163. doi: 10.1016/j.saa.2020.119163.

[19] Nasr JJM, Al-Shaalan NH, Shalan SM. Sustainable environment-friendly quantitative determination of three anti-hyperlipidemic statin drugs and ezetimibe in binary mixtures by first derivative Fourier transform infrared (FTIR) spectroscopy. Spectrochim Acta A Mol Biomol Spectrosc. 2020;237:118332. doi: 10.1016/j.saa.2020.118332.

[20] El-Bagary RI, ElKady EF, Kadry AM. Spectrofluorometric determination of certain antihyperlipidemic agents in bulk and pharmaceutical preparations. J Spectroscopy. 2012;27:83–92. doi: 10.1155/2012/913913. Article ID 913913.

[21] Abbas NS, Derayea SM, Omar MA, Saleh GA. TLC-spectrodensitometric method for simultaneous determination of dapagliflozin and rosuvastatin in rabbit plasma: stability indicating assay and kinetic studies. RSC Adv. 2020;10(67):40795–805. doi: 10.1039/d0ra05628f.

[22] Trivedi HK, Patel MC. Development and validation of a stability-indicating RP-UPLC method for determination of rosuvastatin and related substances in pharmaceutical dosage form. Sci Pharm. 2012;80(2):393–406. doi: 10.3797/scipharm.1201-09.

[23] Mammone FR, Zanitti L, Puxeddu M, La Regina G, Silvestri R, Borioni A, et al. A novel validated UHPLC method for the estimation of rosuvastatin and its complete impurity profile in tablet formulations. Molecules. 2023;28:431. doi: 10.3390/molecules2801043.

[24] Attimarad M, Alkadham A, Almosawi MH, Venugopala KN. Development of rapid and validated RP-HPLC method for concurrent quantification of rosuvastatin and aspirin form solid dosage form. Indian J Pharm Edu Res. 2018;52(1):151–8. doi: 10.5530/ijper.52.1.17.

[25] Gholve R, Pekamwar S, Wadher S, Kalyankar T. Stability-indicating RP-HPLC method development and validation for simultaneous estimation of telmisartan and rosuvastatin calcium in bulk and in tablet dosage form. Future J Pharm Sci. 2021;7:224. doi: 10.1186/s43094-021-00369-2.

[26] Rathinam S, Santhana LK. Analytical quality by design approach for estimating Rosuvastatin calcium in pharmaceutical formulation by green HPLC method: Ecologically evaluated and stability-indicating. J Appl Pharm Sci. 2021;11(11):150–60. doi: 10.7324/JAPS.2021.1101119. ISSN 2231-3354.

[27] Hussain A, Zakria M, Tariq SA, Siraj S, Khan A, Khattak BG, et al. Simultaneous analysis of atorvastatin and rosuvastatin by LC-MS: development, validation, and application of the proposed method to analysis of atorvastatin pharmacokinetics in Pakistani population. Pharm Chem J. 2022;56:1149–56. doi: 10.1007/s11094-022-02766-0.

[28] Attimarad M, Venugopala KN, Shafi S, Balgoname AA, Altaysan AI. Smart spectrophotometric method development for simultaneous estimation of antidiabetic drugs in formulations. Indian J Pharm Edu Res. 2022;56:224–31. doi: 10.5530/ijper.56.1.26.

[29] Attimarad M, Venugopala KN, Nair AB, Sreeharsha N, Molina EIP, Kotnal RB, et al. Environmental sustainable mathematically processed UV spectroscopic methods for quality control analysis of remogliflozin and teneligliptin: Evaluation of greenness and whiteness. Spectrochim Acta A Mol Biomol Spectrosc. 2022;278:121303. doi: 10.1016/j.saa.2022.121303.

[30] Attimarad M, Venugopala KN, Nair AB, Sreeharsha N, Deb PK. Experimental design approach for quantitative expressions of simultaneous quantification of two binary formulations containing remogliflozin and gliptins by RP-HPLC. Separations. 2022;9:1–15. doi: 10.3390/separations9020023.

[31] Vetapalem R, Yejella RP, Atmakuri LR. Development and validation of a stability indicating RP-HPLC method for simultaneous estimation of teneligliptin and metformin. Turk J Pharm Sci. 2020;17:141–7. doi: 10.4274/tjps.galenos.2018.16768.

[32] Kumar TNVG, Vidyadhara S, Narkhede NA, Silpa YS, Lakshmi MR. Method development, validation, and stability studies of teneligliptin by RP-HPLC and identification of degradation products by UPLC tandem mass spectroscopy. J Anal Sci Technol. 2016;7:27. doi: 10.1186/s40543-016-0107-4.

[33] Park J, Kim K, Park J. Development of a liquid chromatography/tandem-mass spectrometry assay for the simultaneous determination of teneligliptin and its active metabolite teneligliptin sulfoxide in human plasma. Biomed Chromatogr. 2020;34:e4721. doi: 10.1002/bmc.4721.

[34] Patel F, Dalwadi P, Patel D, Mehta N. Development and validation of RP-HPLC method for simultaneous estimation of teneligliptin hydrobromide hydrtae and rosuvastatin calcium in synthetic mixture. Int J All Res Edu Scientific Method. 2021;9(4):2712.

[35] Mukhtiyarmiya SJ, Sarkar S. Stability indicating analytical method development and validation for simultaneous estimation of teneligliptin hemihydrate hydrobromide and rosuvastatin calcium in synthetic mixture. World J Pharma Pharmaceut Sci. 2022;11(1):1916–52.

[36] Vyas A, Godhaniya J, Patel A, Patel A, Patel N, Shah S, et al. Development and validation of UV-spectroscopic first order derivative method for simultaneous estimation of rosuvastatin calcium and teneligliptin hydrobromide hydrate in synthetic mixture. Chem Methodol. 2021;5(4):317–23. doi: 10.22034/chemm.2021.131260.

[37] Kamal AH, El-Malla SF, Hammad SF. A review on UV spectrophotometric methods for simultaneous multicomponent analysis. Eur J Pharm Med Res. 2016;3:348–60.

[38] Salinas F, Nevado JJB, Mansilla AE. A new spectrophotometric method for quantitative multicomponent analysis resolution of mixtures of salicylic and salicyluric acids. Talanta. 1990;37:347–51.

[39] Chohan MS, Attimarad M, Venugopala KN, Nair AB, Sreeharsha N, Molina EIP, et al. Sensitivity enhanced ecofriendly UV spectrophotometric methods for quality control of telmisartan and benidipine formulations: comparison of whiteness and greenness with HPLC methods. Int J Environ Res Public Health. 2022;19:7260. doi: 10.3390/ijerph19127260.

[40] Attimarad M, Chohan MS, Venugopala KN, Nair AB, Sreeharsha N, Molina EIP, et al. Mathematically processed UV spectroscopic method for quantification of chlorthalidone and azelnidipine in

bulk and formulation: evaluation of greenness and whiteness. J Spectro. 2022;2022:1–13.doi: 10.1155/2022/4965138.

[41] Saleh SS, Lotfy HM, Tiris G, Erk N, El-Naem OA. The power of high impact amplitude manipulation (HIAM) technique for extracting the basic spectra of two fixed-dose combinations (FDC)-spectrophotometric purity analysis via spectral contrast angle. Spectrochim Acta Part A. 2022;273:121036. doi: 10.1016/j.saa.2022.121036.

[42] Raynie D, Driver J. Green assessment of chemical methods. 13th Annual Green Chemistry and Engineering Conference. Maryland; 2009.

[43] Płotka-Wasylka J. A new tool for the evaluation of the analytical procedure: green analytical procedure index. Talanta 2018;181:204–9. doi: 10.1016/j.talanta.2018.01.013.

[44] Pena-Pereira F, Wojnowski W, Tobiszewski M. AGREE – analytical GREEnness metric approach and software. Anal Chem. 2020;92:10076–82. doi: 10.1021/acs.analchem.0c01887.